ELSEVIER

Coordination Chemistry Reviews
150 (1996) 221–242

COORDINATION CHEMISTRY REVIEWS

Chapter 8
Considerations on high resolution solid state NMR in paramagnetic molecules

S. Aime, I. Bertini, C. Luchinat

Contents

8.1. Introduction

In Chapter 2 reference was made to isooriented molecules in a solid sample, as far as the shifts are concerned. This allowed us to treat the I–S dipolar coupling through a simple equation (Eq. (2.12)). In solution the average value is needed and, in the assumption of isotropic χ (and g) values, the I–S dipolar coupling averages zero (see Section 2.2.2). The contact coupling is essentially orientation independent (see, however, Section 8.2.1.).

The ideal case of isooriented molecules in an ordinate tridimensional arrangement is rarely encountered in real solids. In general the unit cell contains more than one molecule, and the number of resonances in the solid state spectrum corresponds then to the number of magnetically inequivalent sites [1].

Actually, the effects of paramagnetic centers in solids are even larger than those in liquids because of the absence of motional averaging. The paramagnetic shift is considerably orientation dependent (see Section 2.2.2). In a polycrystalline sample the resulting powder pattern is broadened by the different orientations of the crystals. Further complications arise when a nucleus senses more than one paramagnetic metal center in concentrated polycrystalline materials.

PII S0010-8545(96)01252-0

Nuclei in the diamagnetic solid state are characterized by short T_2 and long T_1. This is because near-zero frequencies of lattice magnetic fields oscillating along the external magnetic field direction provide efficient transverse relaxation and not longitudinal relaxation (Section 3.2). As a consequence, the lines are broad and the recycle time has to be long when accumulating the FIDs. The paramagnetic contribution adds to the linewidth, thus making the spectral resolution worse, whereas a decrease in T_1 is of help in that fastest recycling is possible. Of course, dipolar relaxation mechanisms are orientation dependent, since they depend on the square of the dipolar coupling energy of Eq. (2.12), modulated by τ_s. By rotating the crystal in three orthogonal directions the full anisotropic relaxation tensor is obtained.

Among the most suitable systems to be investigated are those containing lanthanide ions (except gadolinium(III)) since these ions have the shortest electronic relaxation times.

For polycrystalline samples, all molecular orientations are present in the ensemble and the absorption is the envelope of the absorptions for each orientation. As in the EPR case, the absorption curve looks like that reported in Fig. 8.1(A) for an axially symmetric system. The spectrum in derivative mode (Fig. 8.1(B)) shows the shifts for the parallel and perpendicular cases. It is intuitive that the absorption lines are very broad, and it may be difficult to distinguish between sets of signals. Sometimes it may be convenient to lower the temperature, in such a way that the hyperfine shift is larger than the linewidths.

If the sample, either single crystal or powder, is allowed to rotate about an axis at the angle of 54°44′ with the magnetic field axis (the so-called magic angle), the paramagnetic dipolar shift (as well as all other dipolar interactions which do not involve the unpaired electrons) averages zero (or to the well-known pseudocontact term, see Section 2.2.2).

This is because, by rotating the sample at 54°44′, all interactions at a generic γ angle (as defined in Fig. 2.6) average a γ angle of 54°44′, and $3\cos^2\gamma - 1 = 0$ for that γ angle. This technique is the well-known magic angle sample spinning (MASS) (Fig. 8.2). MASS averages the orientation-dependent components of the interaction yielding reasonable resolution in the solid. However, spinning at frequencies ν_R smaller than the frequency spread of the interaction to be removed results in the isotropic (average) peak being flanked by a series of spinning sidebands (SSBs) separated by the spinning frequency.

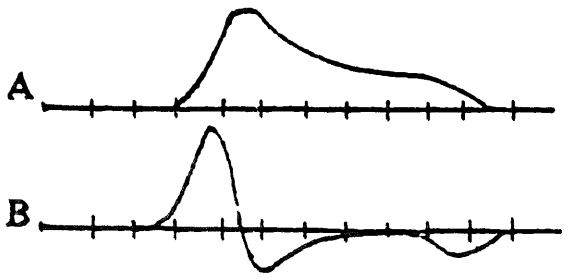

Fig. 8.1. Typical solid state NMR spectra of an $I = 1/2$ system experiencing dipolar interactions. The absorption (A) and first derivative (B) modes are shown.

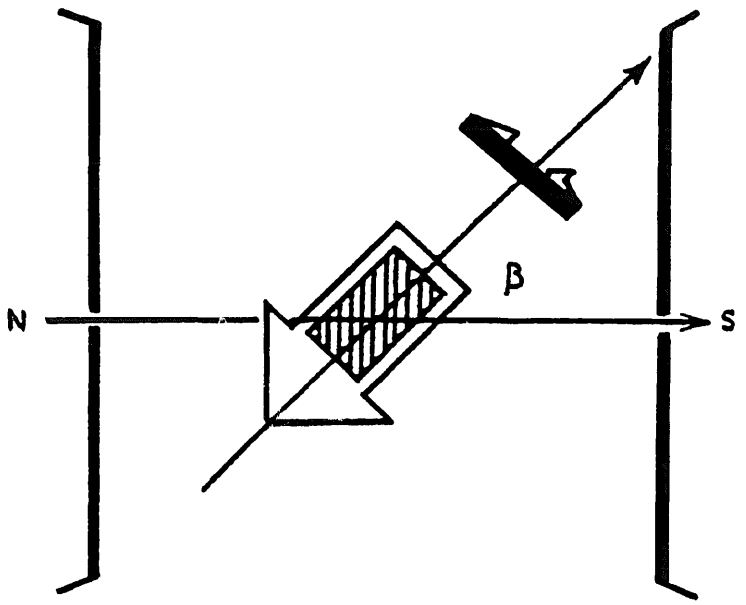

Fig. 8.2. Schematic representation of the experimental arrangement for sample spinning illustrated with a rotor of the Andrew–Beams type. In MASS, $\beta = 54°44'$.

Thus sidebands of significant intensity cover a frequency range comparable with the static linewidth Δ, and accordingly their number will be ca. Δ/ν_R. This behavior is due to the fact that rapid sample rotation at the magic angle causes a modulation of the spin interactions manifesting itself in the form of sidebands.

The relative intensities of the sidebands are proportional to the intensity of the powder spectrum (such as that shown in Fig. 8.1(a)) at their frequencies. The requirement to observe narrow central lines (+SSBs) becomes $T_R < T_2$, where $T_R = 1/\nu_R$ is the period of rotation. The requirement is essentially equivalent to the requirement $\tau_c < T_2$ for motional narrowing by molecular reorientation in solution. When the linewidth of the individual sidebands exceeds the spinning speed, the resonance is no longer broken up into spinning sidebands by magic-angle rotation, and thus it is essentially the same as that of the powder sample, i.e. difficult to observe. In paramagnetic systems it may be impossible to rotate at a speed larger than the spreading of the dipolar shifts, at least for protons since they have large magnetic moments: therefore, the combination of insufficient spinning speed and large intrinsic linewidths may prevent the observation of MASS spectra.

We note that, when dealing with spectra of polycrystalline paramagnetic samples, depending on the degree of refinement of the information, one may consider that there is no magnetic anisotropy and therefore the interpretation can be made on the basis of a cylindrical symmetry as imposed by the magnetic field. For more refined studies (possibly with the aid of MASS or single crystal data), and when appropriate, Eq. (2.12), which is valid for an axially anisotropic χ tensor, can be used to obtain information on the internal tensor. Under these circumstances, the powder spectrum results are rhombic. In principle, an equation more general than Eq. (2.12) can be used, which includes rhombic components.

8.2. Polycrystalline ^{1}H and ^{19}F NMR studies

These studies deal with the static spectra of polycrystalline materials containing ^{1}H and ^{19}F nuclei, that have large γ value and usually high concentration in the studied compounds, having 100% natural abundance. The linewidth of their resonance is dominated by the large dipolar interactions, and a single "wide line" resonance is invariably observed in their spectra.

The experimentally determined parameters from these spectra are the overall width of the line, expressed as the so-called second moment, and the relaxation times. The second moment (M_2), is the mean square width of the line, measured (as shown in Fig. 8.3) as:

$$M_2 = \int_{-\infty}^{+\infty} (\omega - \langle\omega\rangle)^2 f(\omega)\, d\omega \Big/ \int_{-\infty}^{+\infty} f(\omega)\, d\omega \tag{8.1}$$

where $\langle\omega\rangle$ is the average frequency of the line, $f\langle\omega\rangle$ is its shape, and the denominator is a normalization factor.

The second moment may be predicted in terms of the average effect of the pairwise dipolar interactions summed over the crystal. For a homonuclear system it is given by

$$M_2 = \frac{3}{4}\hbar^2\gamma^4 I(I+1)\sum_{ij}\frac{(3\cos^2\gamma_{ij}-1)^2}{r_{ij}^6} \tag{8.2}$$

where γ_{ij} is the angle between the field direction and the internuclear vector r_{ij}. For a polycrystalline sample it is possible to average $(3\cos^2\gamma_{ij}-1)^2$ over all directions

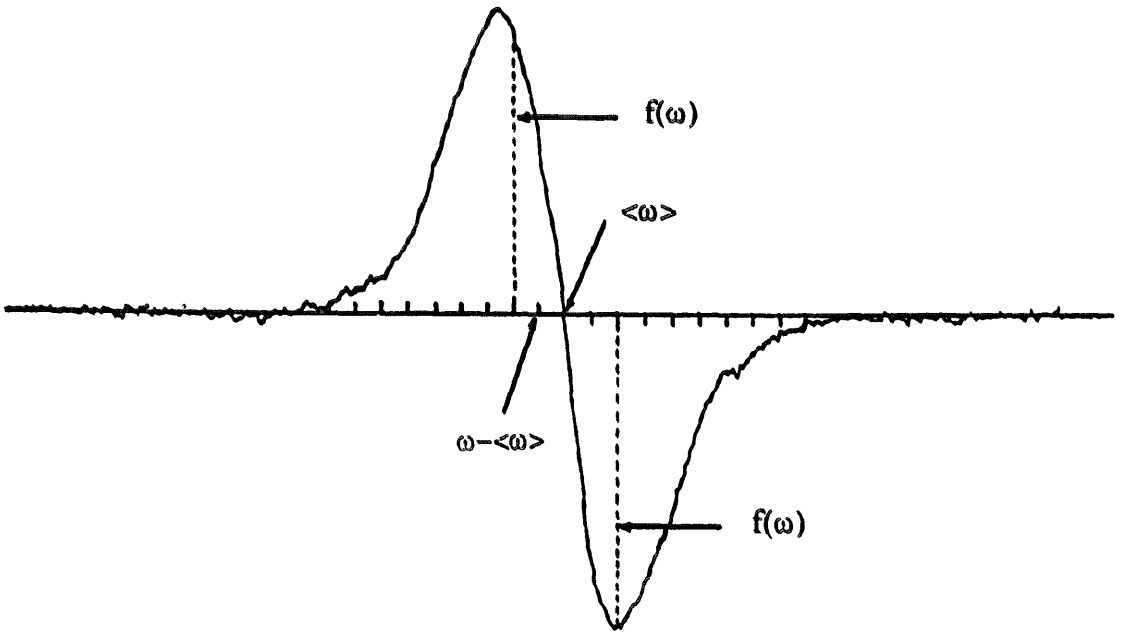

Fig. 8.3. Schematic representation of the parameters of Eq. (8.1) used in the measurement of the experimental second moment parameters [1].

to $\frac{4}{5}$. Thus Eq. (8.2) simplifies to:

$$M_2 = \frac{3}{4} h^2 \gamma^4 I(I+1) \sum_{ij} \frac{1}{r_{ij}^6} \tag{8.3}$$

For convenience, the second moment is often divided into an intramolecular part (arising from interactions within the molecule) and an intermolecular part (arising from interactions with surrounding molecules). Thus, M_2 can be determined from the knowledge of the crystal structure. The occurrence of molecular motions in the solid state causes a partial averaging of the dipolar interactions which gives a narrowing of the spectrum to some intermediate value.

In the case of paramagnetic systems an analogous equation for M_2 may be derived which contains an additional term to account for the occurrence of the unpaired electron spin density. From the fitting of ^{1}H static spectra of paramagnetic uranium(IV) containing species, it was found that

$$M_2 = C(3\cos^2\theta - 1)^2 + D \tag{8.4}$$

where the first term accounts for the ^{1}H–^{1}H dipole–dipole interaction and the additional term D (which increases linearly with T^{-1}) accounts for the paramagnetic interactions [2].

Analogously, information on molecular motions in the solid state may be obtained by variable temperature investigations of linewidths and relaxation times.

8.2.1. ^{1}H NMR powder studies

As stated above, ^{1}H-second moments can be predicted once the intra- and interatomic distances (between magnetically active nuclei) are known. For instance, it was earlier reported that the experimental second moment of the paramagnetic $U(C_8H_8)_2$ (uranocene) is much less than the theoretical second moment predicted in the presence of a rigid lattice [3]. To account for this observation it has been proposed that there must be a low rotational barrier in uranocene which allows independent motion of the two π-rings along their coordination axis. Later the static ^{1}H-variable-temperature NMR spectra of this compound and those of the related $U(C_5H_5)_3Cl$ have been thoroughly investigated by McGarvey and Nagy [2]. As shown in Fig. 8.4 there is a marked linewidth variation upon changing the temperature; in $U(C_5H_5)_3Cl$ the random reorientation of the molecule is so rapid that above 220 K it has a liquid-like resonance.

Both systems show a distinctly anisotropic shape at all temperatures which, as mentioned in Section 8.1, can be interpreted as due to an axial magnetic anisotropy. From the analysis of the lineshapes it is possible to extract the principal tensor components since X-ray structural data are available. The values obtained for both $\Delta_{\chi\parallel}$ and $\Delta_{\chi\perp}$ are rather small due to the fact that the angle between the vector joining H and U and the $\chi_\parallel$ axis is close to the "magic angle" which makes $(3\cos^2\theta - 1) = 0$ in Eq. (2.14).

Furthermore, from a detailed analysis of the lineshape of the ^{1}H-static spectra, it

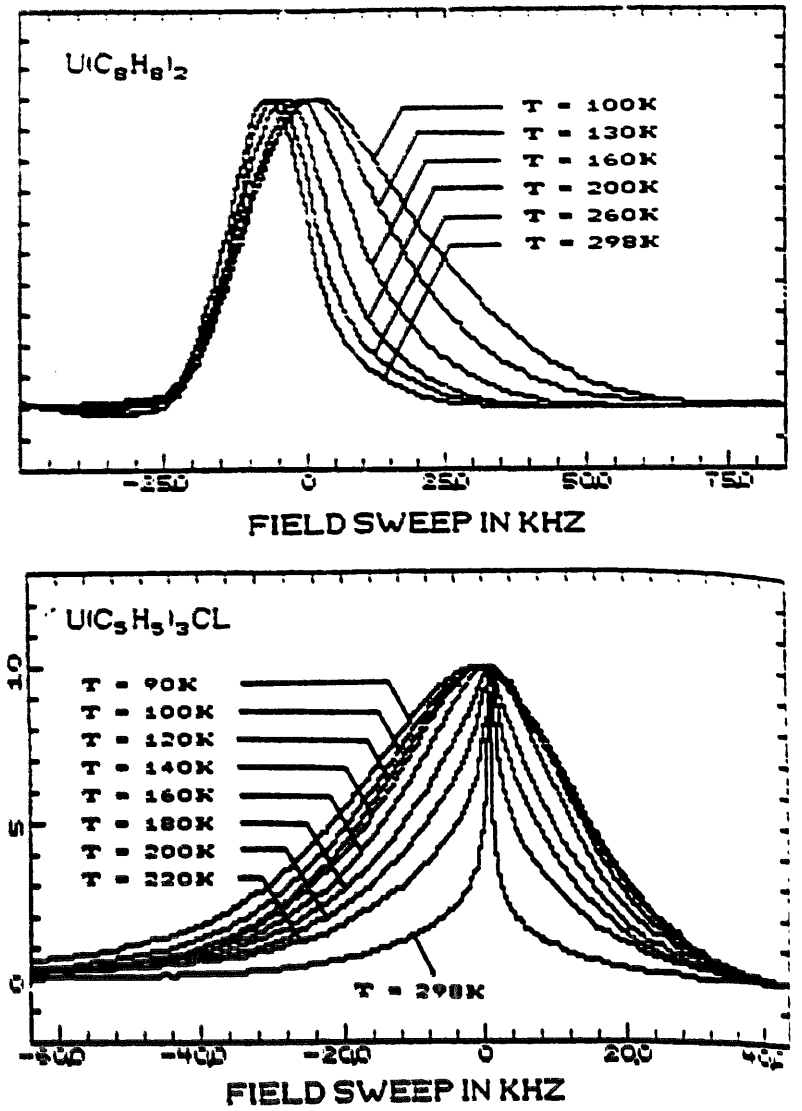

Fig. 8.4. Absorption ^1H NMR spectra at 90 MHz for uranocene and $U(C_2H_5)_3Cl$ powders at different temperatures. Sweep scale has the magnetic field increasing to the right [2].

has been shown that there is an anisotropic contribution to the Fermi contact term. At first glance this may be a surprise to many as the Fermi contact interaction, dealing with s electrons, is believed to be isotropic. However, as these results point out for the first time, the Fermi contact interaction can be anisotropic when the orbital angular momentum is not quenched as is the case of lanthanide and actinide systems (except for the f^7 configuration). This subject has been treated in Section 2.2.1.

8.2.2. ^{19}F NMR studies: the powder LnF_6^{3-} case

These systems are magnetically concentrated. In this case the resonating nucleus is coupled to more than one metal ion, and the following equation should be used

for the shift in every direction [4]:

$$\delta^{hyp} = \frac{1}{\hbar\gamma_I B_0}\left(\sum_I A_I \langle S_z\rangle_J + g_e\mu_B \sum_i (3\cos^2\gamma_i - 1) \Big/ r_i^3 \langle J_z\rangle\right) \tag{8.5}$$

where the sum is extended to all metal ions at a distance r_i, and where all the other symbols have the usual meaning. A general consequence of this multiple hyperfine interaction is that the pattern of the powder spectrum is not axial anymore. This can be visualized by considering that, when $\gamma = 0$ or 90° for one of the metal–nucleus vectors, i.e. when the shift contributed by the metal ion is at an extreme value, the other γ has a different value, and contributes a non-extremal shift. It may be convenient [4] to define an asymmetry parameter Δ as given by

$$\Delta = \frac{H_z - H_y}{H_z - H_x} \tag{8.6}$$

where H_x, H_y and H_z are the principal values of the total dipolar shift tensor. The spectra are axial in the limit cases $\Delta = 0$ or $\Delta = 1$, and rhombic in all other cases.

The resulting calculated spectra are shown in Fig. 8.5. It has been proposed that consideration of the two nearest metal ions is often a reasonable approximation. As an example to illustrate the use of ^{19}F NMR of paramagnetic compounds we report the case of $M_2M'LnF_6$ where the fluoride ions occupy sites of tetragonal symmetry (4*mm*). The ^{19}F spectrum is shown in Fig. 8.6. The spectrum is axial, on account of the spatial arrangements of the various ions.

The analysis of the data have allowed the authors to factorize the metal-centered dipolar shift and the ligand-centered dipolar shift; the latter contribution has been further factorized into a direct spin transfer and spin polarization effects [5]. It is interesting to note that unpaired spin density onto fluoride 2p orbitals, responsible for ligand-centered dipolar shifts, arises from both direct and spin polarization mechanisms. The two mechanisms are both important for lanthanides in the second half of the series, whereas spin polarization mechanisms seem more important in the first half of the series. The result could only be achieved by the analysis of solid state spectra, as the solution spectra would have provided only the isotropic contribution, which is obtained from the powder spectra as the weighted average between the parallel and the perpendicular contributions, $(H_z + 2H_\perp)/3$.

8.3. ^2H NMR studies of single crystals and powders

The ^2H nucleus has a nuclear spin, $I = 1$, and a quadrupolar moment of $Q = 2.8 \times 10^{-31}$ m^2, which interacts with the field gradient at the position of the deuteron. As the quadrupole splitting for deuterons in crystals (about 200 kHz) is generally larger than the linewidth (about 1 kHz), the absorption lines of non-equivalent deuterons in crystals can be observed separately. Thus, as shown in Fig. 8.7(B), each deuteron appears as a doublet spaced by $\frac{3}{8}(\cos^2\theta - 1)\chi$ for a given orientation θ of the electric field gradient in B_0 where $\chi = e^2Qq_{zz}/h$ is the quadrupole coupling constant.

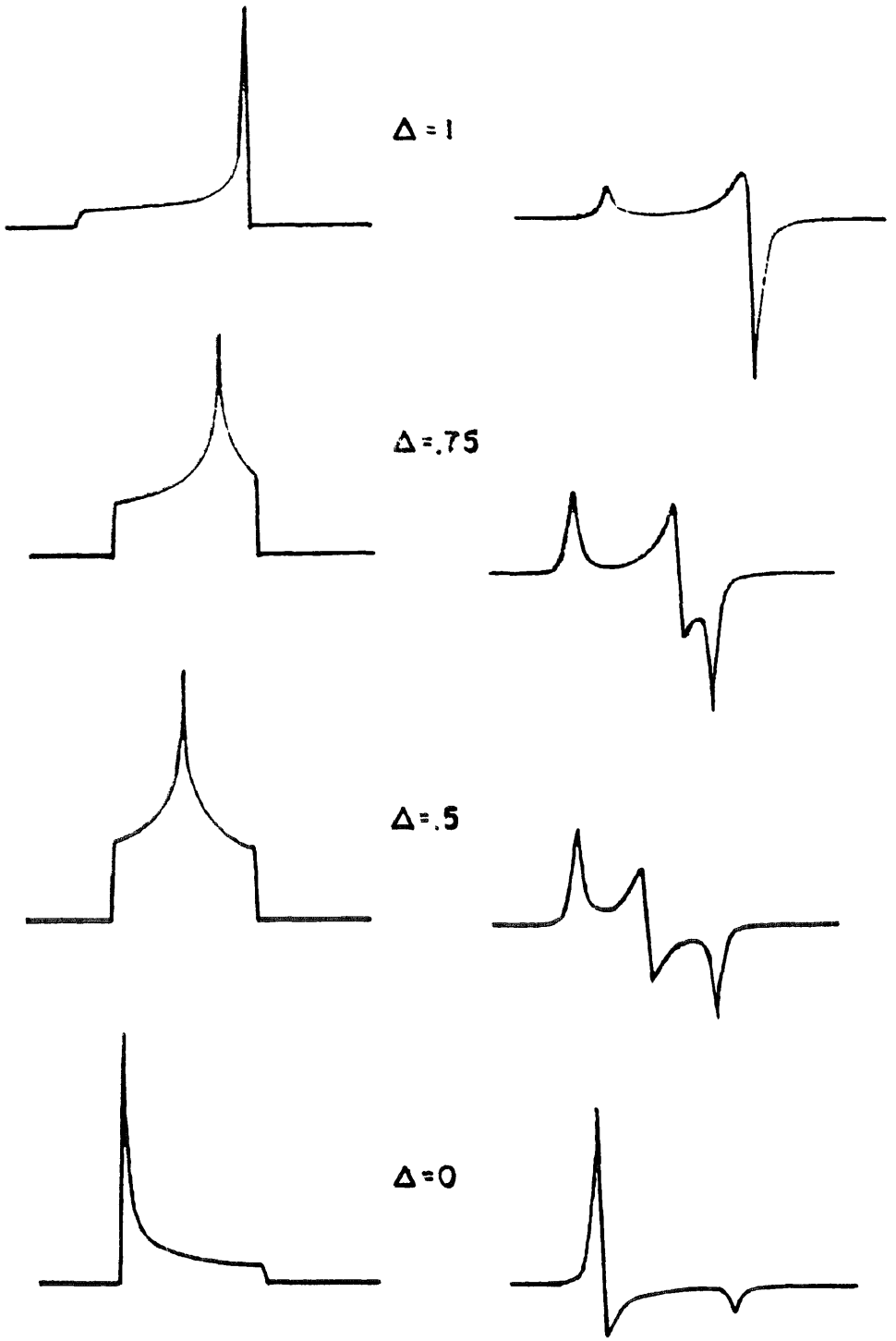

Fig. 8.5. Calculated absorption and derivative NMR spectra as a function of the asymmetry parameter Δ [4].

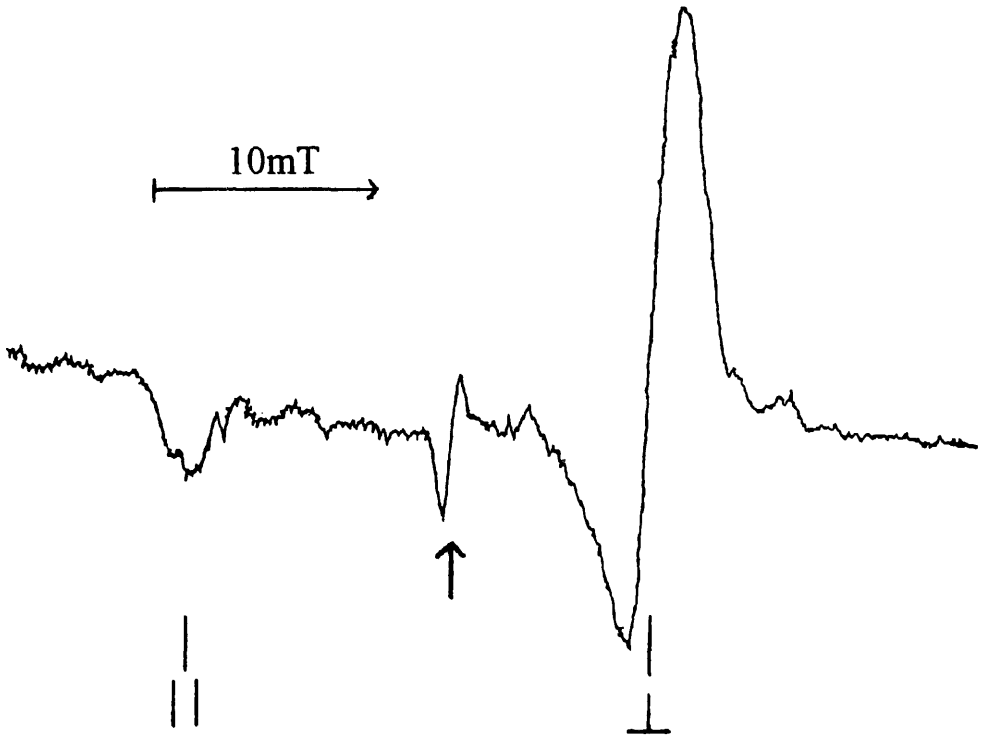

Fig. 8.6. Room temperature first derivative ^{19}F NMR spectrum of Rb_2NaErF_6. The spectrum is axial. The sharp line indicated by an arrow is due to external ionic fluoride [5].

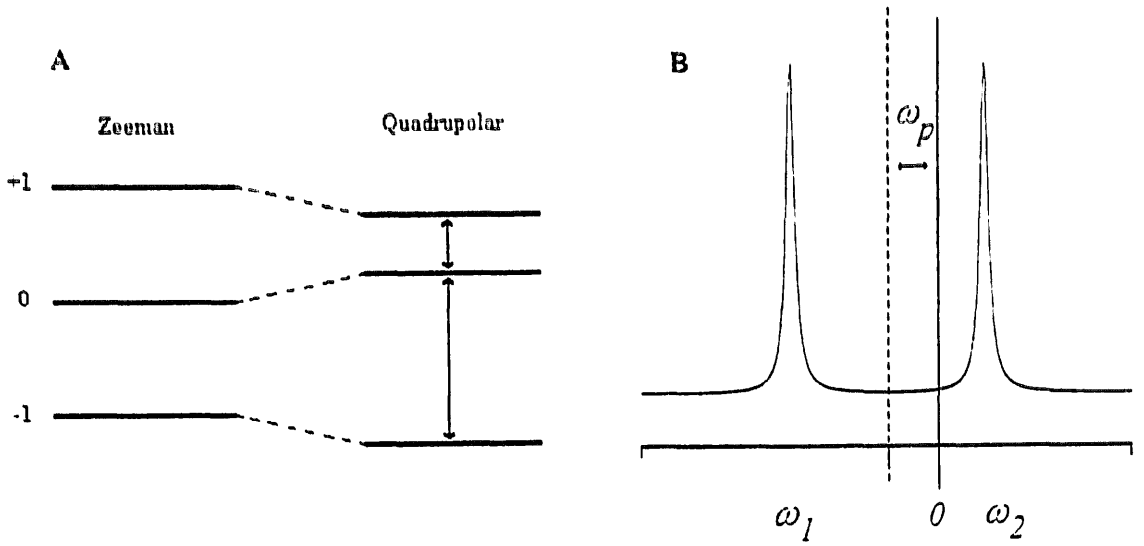

Fig. 8.7. (A) Schematic representation of the energy levels for a deuteron ($I = 1$) resulting from the Zeeman interaction with the magnetic field and with the quadrupole moment of the nucleus. (B) Spectral splitting pattern for a deuteron in a paramagnetic system. ω_p is the displacement from the diamagnetic position by the interaction with the unpaired electrons.

In a paramagnetic species, the center of this doublet is shifted by the quantity ω_p from the position held by a corresponding diamagnetic system. For instance, ten pairs of lines were separately observed [6] in the low temperature (130 K) spectrum of $CuSO_4 \cdot (^2H_2O)_5$ corresponding to five non-equivalent stationary water molecules. At temperatures above room temperature, five pairs of lines are observed; these are shown to result from fast molecular reorientation about the bisecting axis of each water molecule.

Furthermore, an experimental procedure has been reported to assign each quadrupolar doublet [7]. In Fig. 8.8 the spectrum of a single crystal of $Cu(^2H_2O)_5^{2+}$ is shown for an arbitrary orientation which allows the observation of six signals (three quadrupolar split doublets). If now we selectively irradiate the $0 \rightarrow 1$ transition, also the $0 \rightarrow -1$ transition will change in intensity due to the change in population of the $M_I = 0$ level. Through spectral difference, selective irradiation of one signal allows the detection of its quadrupolar partner. From the same figure, the three quadrupolar doublets, centered at 67.3, 30.8 and 6.3 kHz, are clearly evident.

A huge number of investigations have been carried out on diamagnetic systems by ^2H NMR of static samples and this technique has provided relevant information in the characterization of molecular motions in the solid state. This is essentially dependent on the size of ^2H quadrupole interaction which is well matched to the

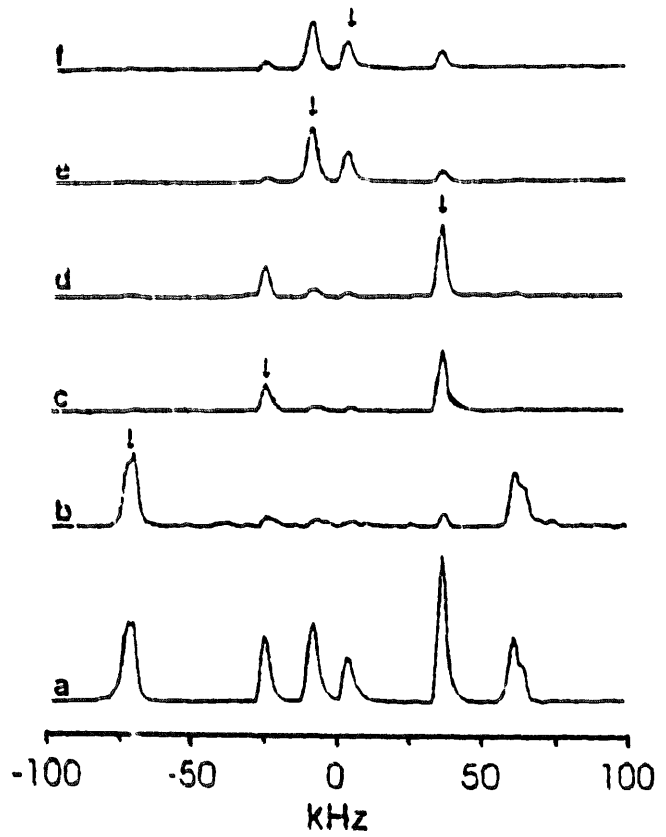

Fig. 8.8. ^2H NMR spectra of a single crystal of $CuSO_4 \cdot (^2H_2O)_5$ (a). Difference spectra (b)–(f) are taken by selectively irradiating at the frequencies marked by arrows [7].

timescale of many dynamic processes which occur in the solid state. For example, a common value of e^2qQ/h is about 2×10^5 Hz; thus, molecular motions which occur on a 10^{-3} to 10^{-7}s timescale will influence the deuterium spectral lineshapes.

Methods for recording the rather wide (about 250 kHz) ^{2}H NMR spectra involve Fourier transformation of a two-pulse quadrupole echo. The signal generated by the first pulse is refocused by the second to form an echo, and Fourier-transformed beginning at the echo peak. In order to excite ^{2}H-spectra, uniformly short (1.5–2.0 μs) pulses are required, and the signal must be digitized every microsecond or less in order to accurately locate the echo peak.

A system which has been widely investigated by ^{2}H NMR spectroscopy is represented by the trinuclear derivative $[Fe_3O(COOCH_3)_6L_3]S$ where L is a nitrogen donor ligand and S is a solvate organic molecule (Fig. 8.9) [8]. These are mixed-valence complexes (two Fe(III) and one Fe(II)) in which the intramolecular electron transfer is dramatically affected by changing the solvate molecule in the crystal cell.

Evidence for the motion of the solvate molecule at room temperature has been gained when the solvate molecule is a deuterated benzene by carrying out a single-crystal ^{2}H NMR study. Rotations were carried out about three orthogonal axes. At every setting of the single crystal only a single quadrupole-split doublet is seen. It is clear that the $C_6{}^2H_6$ molecule is rapidly rotating about a six-fold axis to make all deuteron sites equivalent. Furthermore, it has been shown that reorientation about

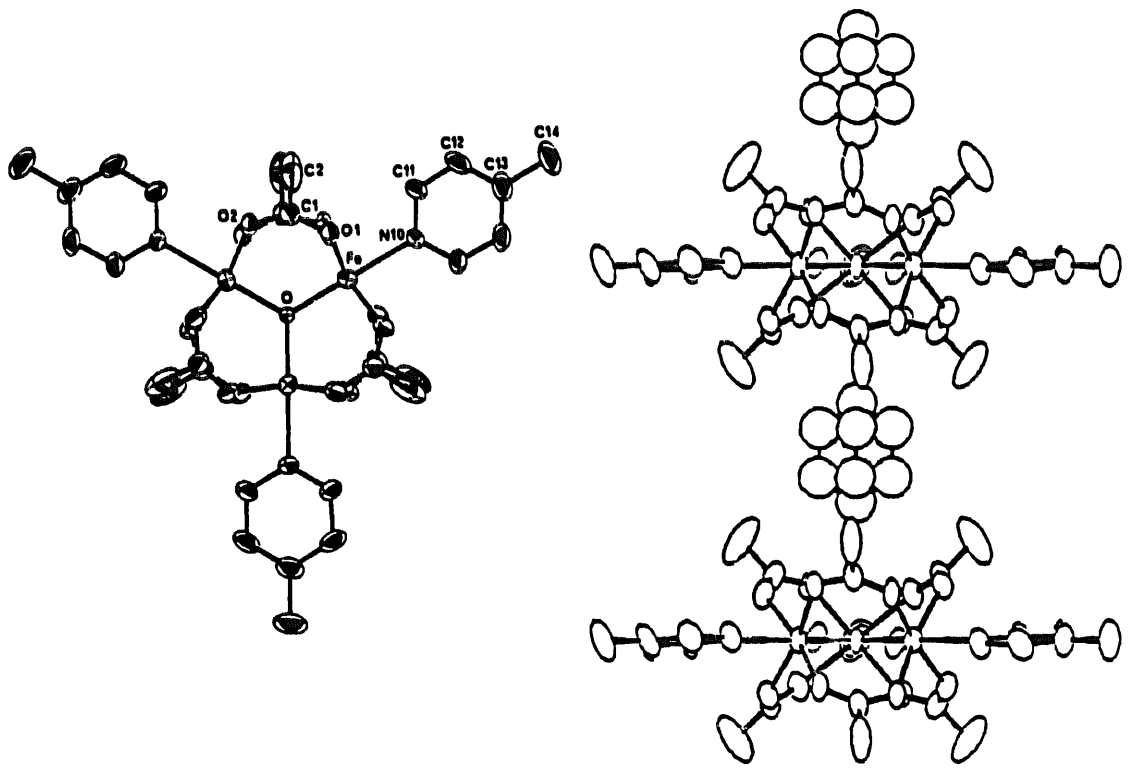

Fig. 8.9. ORTEP of the molecular structure of $Fe_3O(O_2CCH_3)_6$(4-Mepy)$_3$ in the benzene solvate compound and view of the stacking along the c axis [8].

the C_3 axis along the molecular stacks is also present in addition to the rotation about the six-fold axis.

An illustration of the potential of ^2H lineshape to report on the molecular dynamics and electronic properties of a paramagnetic system is shown by the ^2H NMR study at variable temperature of powder $NdCl_3 \cdot 6^2H_2O$ (Fig. 8.10) [9].

On the basis that the electron spin-lattice relaxation rate is much higher than the Larmor frequency and that electron–deuteron interaction is purely dipolar, the simulation of VT ^2H NMR spectra at variable temperature has allowed the evaluation of the rate of two-fold flips of ^2H_2O molecules about the $^2HO^2H$ bisector.

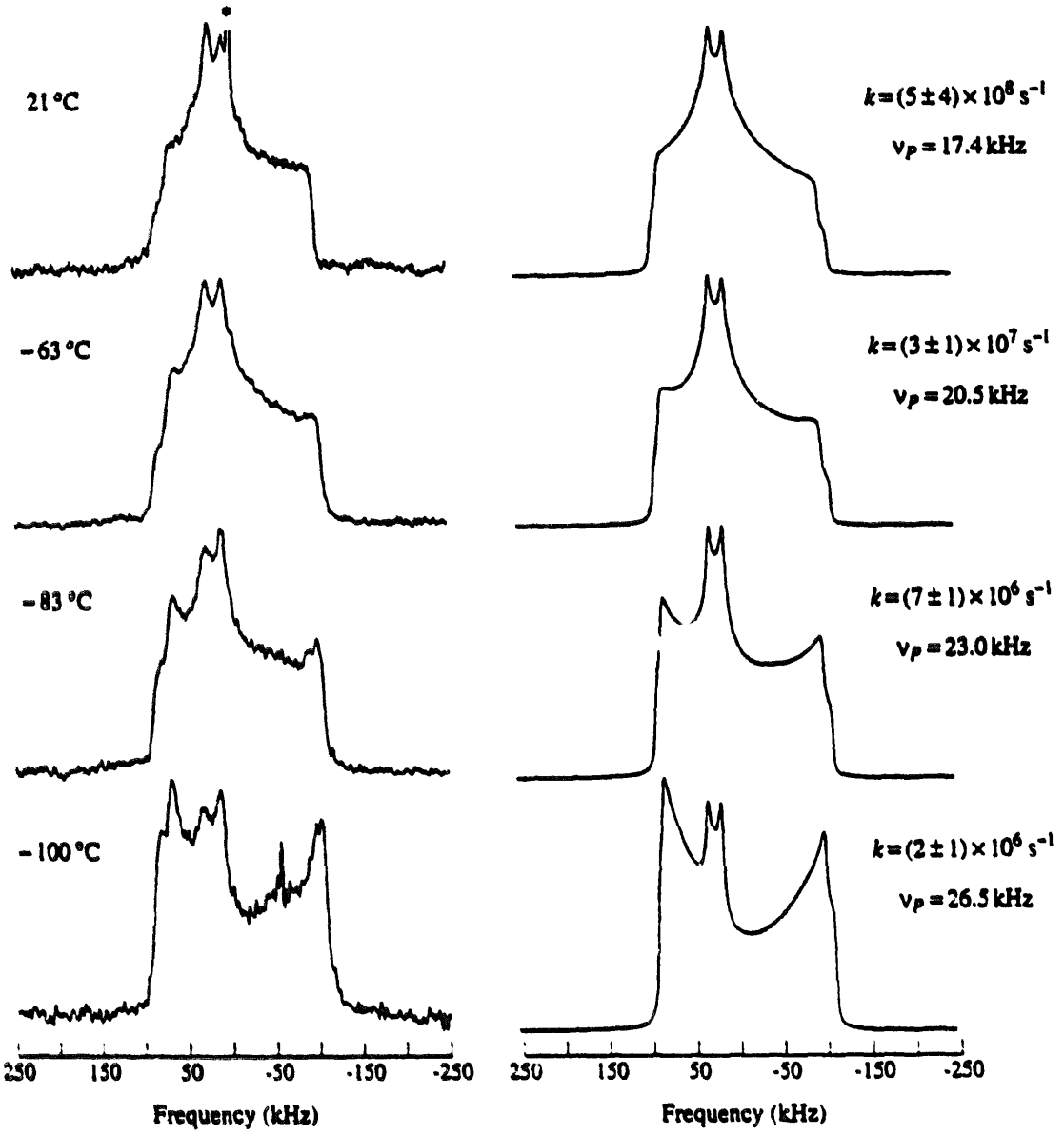

Fig. 8.10. Deuterium NMR spectra (left column) of powder $NdCl_3 \cdot 6^2H_2O$ recorded as a function of temperature at 38.4 MHz (5.9 T). The simulated spectra (right column) are also shown [9].

A best-fit analysis of the rates of 180° flips gives an activation energy 21.4 kJ mol^{-1} which is similar to values found for other diamagnetic hydrated salts.

8.4. MASS NMR spectra

As for diamagnetic solids, also in the case of paramagnetic systems, the MASS experiment is the technique of choice to obtain full advantage of the large armoury of NMR parameters (isotropic and anisotropic shifts, linewidth of the individual SSB, relaxation times). As anticipated above, the large bandwidths of NMR resonances in paramagnetic systems often overcome the possible rotation speeds (up to several kilohertz) and then the resulting MASS NMR spectrum is complicated by the occurrence of a number of SSBs which flank the central resonance.

There are several factors influencing the relaxation parameters of the individual signals (and the relative SSBs): (a) T_1 and T_2 in paramagnetic compounds are, of course, reduced relative to the analogous diamagnetic materials, but, often, as occurs in solution, the electronic relaxation associated with transition metal or lanthanide ions may be too fast to induce significant nuclear relaxation; (b) another source of broadening is caused by the anisotropic bulk magnetic susceptibility, which results from the distribution of internal fields because of the effects of the difference in susceptibility between the sample and the surrounding air, and because of the non-uniform shapes of the particles. Although this broadening is largely averaged out by MASS, it has been found in a number of compounds that second-order effects due to anisotropy in the bulk susceptibility make a major contribution to the linewidths; (c) analogously, chemical inhomogeneities in the sample may cause changes in the anisotropic bulk magnetic susceptibility; (d) an additional source of broadening for proton-containing species arises from the incomplete proton decoupling related to the large spread of ^1H resonances. Then, this contribution to line broadening is not intrinsic but depends on the inability to decouple the proton completely. To reduce homonuclear dipolar coupling to a level where it could be removed by MASS, an extensive replacement of the protons by deuterons has been suggested. Furthermore, the availability of such perdeuterated species allows one to observe proton (and deuteron) spectra under MASS conditions. The advantages related to the use of deuterated derivatives are nicely represented in the set of spectra reported in Fig. 8.11 for Tempol, a largely used spin-label [10].

The shape and the extent of the SSB envelope are determined, besides by the usual contributions (nucleus–nucleus dipolar coupling and electron–nucleus dipolar coupling), also by the chemical shift anisotropy (CSA) of the given resonance and by the anisotropic part of the contact shift and by the magnetic anisotropy tensor. Usually it is the last term that dominates the spinning side band manifold. The contribution from CSA may be independently evaluated from the spectra of an analogous diamagnetic compound. In the presence of a dominant contribution from χ anisotropy, the tensorial components obtained from analysis of the SSB intensities provide an easy route to obtain structural information.

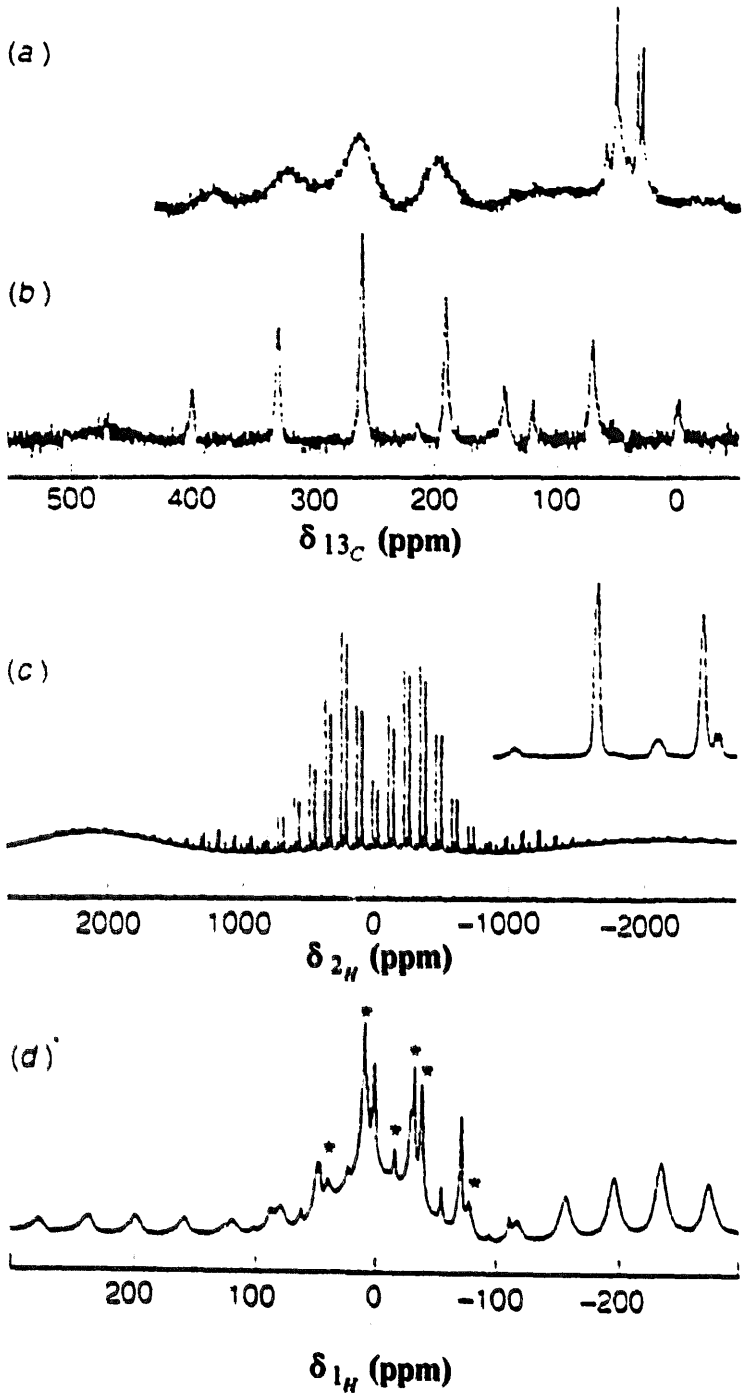

Fig. 8.11. Solid state NMR spectra of Tempol and 97.4%-deuterated [$^2H_{17}$]Tempol: (a) ^{13}C 75.47 MHz CP/MASS of Tempol, $\nu = 4744$ Hz; (b) ^{13}C single pulse MASS of [$^2H_{17}$] Tempol, $\nu = 5304$ Hz; (c) ^2H 46.07 MHz MASS of [$^2H_{17}$] Tempol, $\nu = 5522$ Hz (inset: centerband region); (d) ^1H 300.13 MHz MASS of residual protons in [$^2H_{17}$] Tempol, $\nu = 11\,777$ Hz (centerbands denoted with asterisks). Recorded at 25 °C with 7 or 4 mm double-bearing probes and zirconia rotors. All shifts are relative to TMS [10].

8.4.1. ^{13}C MASS NMR

In analogy to well-established observations in the liquid state, the ^{13}C CP/MASS spectra of paramagnetic compounds are characterized by short relaxation times and large induced paramagnetic shifts. CP/MASS stands for cross polarization magic angle sample spinning and is used when low abundant, low-γ nuclei are under investigation. CP is obtained by exciting the ^{1}H with a 90° pulse, followed by a spin-lock period (see Sections 1.7.4, 7.4 and 7.6); during this period the ^{13}C is irradiated with a B_1 field such that the precession frequency of the ^{13}C nuclei around B_1 matches that of protons in the rotating frame. Under these conditions energy transfer between carbons and protons occurs, and the subsequent ^{13}C FID is enhanced by a factor γ_H/γ_C (i.e. about a factor of four). During acquisition, high power proton decoupling is applied in order to remove H–C dipolar interactions and make MASS requirements less stringent.

The assignment procedures are often based on the carbon relaxation rates rather than on shift. The carbon relaxation is dominated by electron–nuclear dipole–dipole interaction modulated by the electronic relaxation times, which are thus the same as sensed by each carbon atom. The relative comparisons of carbon relaxation times will thus scale as the inverse sixth power of the carbon–paramagnetic center distance.

A difficulty with the interpretation of solid state spectra of paramagnetic complexes is that assignment of carbon resonances cannot be made on the usual benchmark assignment strategies used in solution because the paramagnetically-induced isotropic chemical shifts are large and may be further altered by intermolecular interactions in the crystalline solid. In extreme cases, the resonance of carbon atoms closest to the metal center may be unobservable.

There is a large effect of the temperature on the isotropic chemical shift of ^{13}C resonances in paramagnetic complexes resulting from either (or both) dipolar and contact-shift mechanisms. This was exploited to suggest the first CP/MASS NMR chemical shift thermometer based on the changes of the chemical shift of the carbonyl resonance in samarium acetate tetrahydrate, which obeys the Curie law (i.e. linear with $1/T$) over a wide temperature range (between 333 and 77 K) (Fig. 8.12) [11].

Lanthanide(III) acetates have been thoroughly investigated in order to assess the possibility of using paramagnetic ions in the analysis of solid state structures [12]. Dobson and co-workers [13,14] have shown that deuterated materials exhibit sufficiently good resolution to allow analysis of the large ^{13}C SSB manifold, which results from contributions from CSA (evaluated from the diamagnetic Y(III) analog) and the anisotropic part of the hyperfine shift. For a single nucleus interacting with one paramagnetic center (as is the case of solid solutions of Y(III) acetate doped with a paramagnetic Ln(III) ion) the shift anisotropy will be dominated by coupling to this one paramagnetic moment.

The shift δ will be axial with principal components given by

$$\delta_{\parallel}/\text{ppm} = 2\chi/\pi r^3 \tag{8.5}$$

$$\delta_{\perp}/\text{ppm} = -\chi/\pi r^3 \tag{8.6}$$

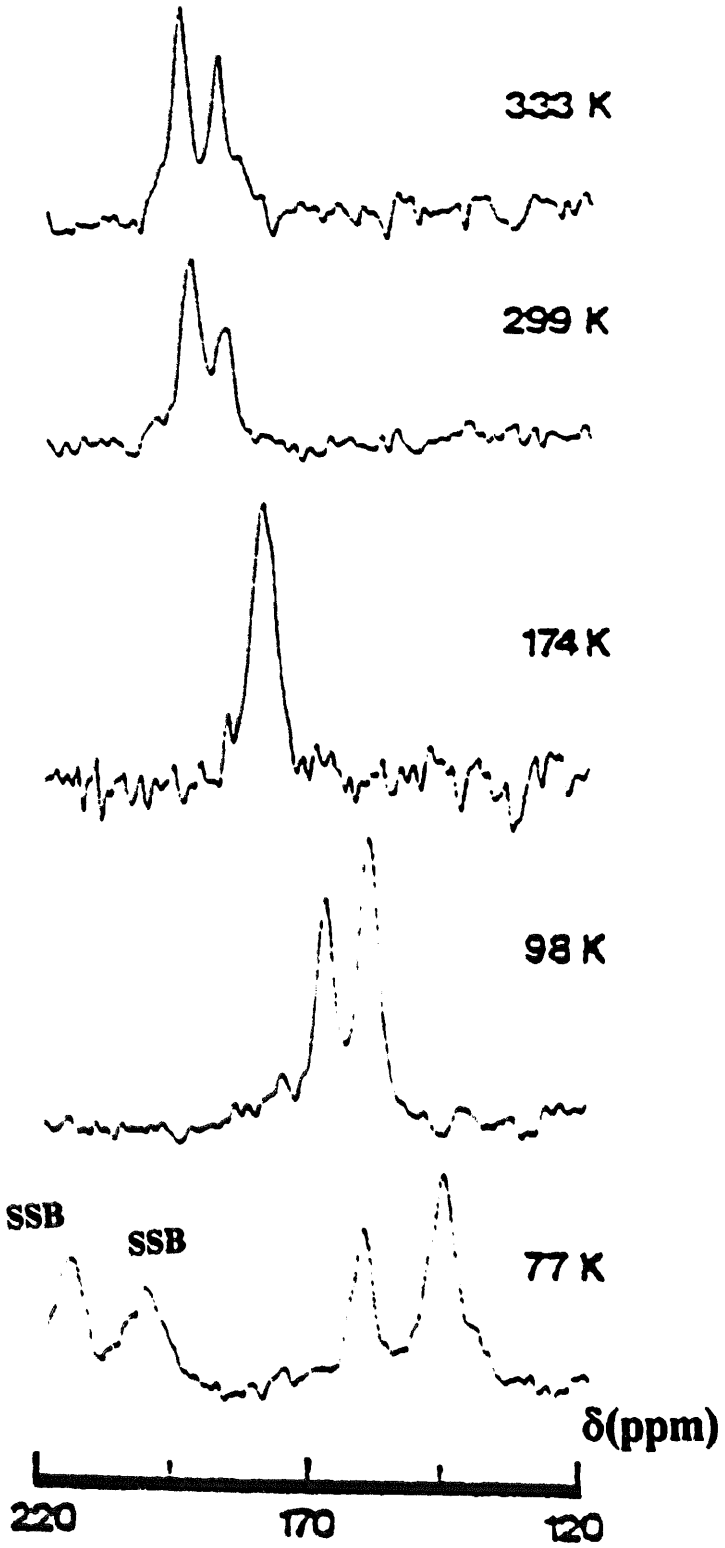

Fig. 8.12. Variable-temperature ^{13}C CP/MASS spectra of the carbonyl region of samarium acetate tetrahydrate between 333 and 77 K–SSB denotes spinning sidebands [11].

A very good agreement between the calculated and X-ray determined r distances has been found by assuming isotropic χ values (i.e. those given for lanthanides by Bleaney) [15].

Haw and Campbell [16] have demonstrated that variable-temperature capability is very important for the study of paramagnetic materials via CP/MASS NMR. The compound $U_3Cl_{12}(C_6Me_6)_2$ (Fig. 8.13(A)) shows a deceptively simple ^{13}C CP/MASS spectrum at room temperature consisting of a single, broad line centered at 8 ppm. One is tempted to rationalize the apparent absence of the aromatic carbon resonance in terms of paramagnetic relaxation. However, two isotropic peaks are observed below room temperature and the chemical shift of one of these is strongly temperature dependent. As shown in Fig. 8.13(B), the SSBs are associated with the signal whose

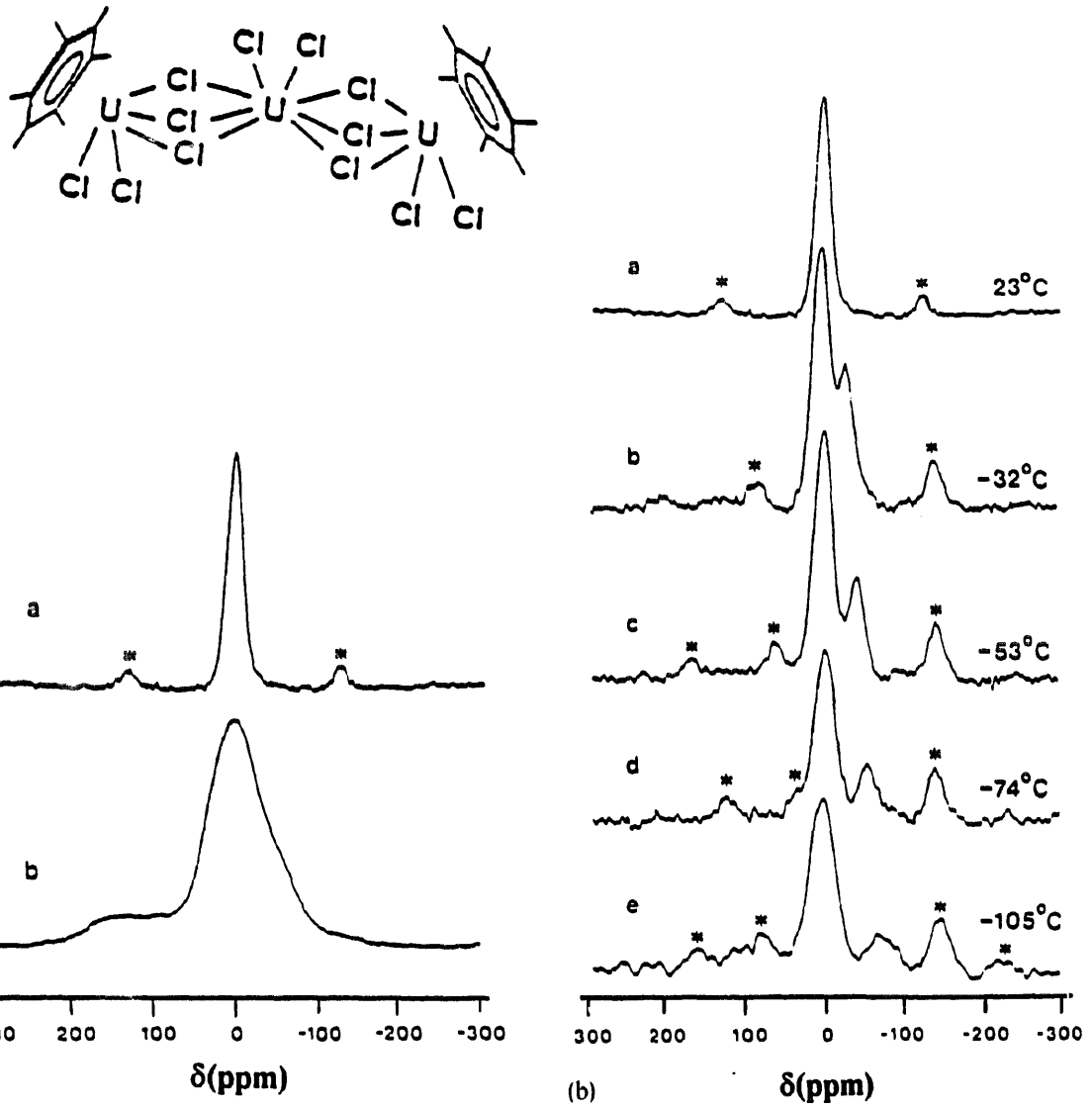

Fig. 8.13. (a) ^{13}C CP/MASS spectrum of $U_3Cl_{12}(C_6Me_6)_2$ at room temperature; * denotes SSBs. (b) ^{13}C NMR spectrum of $U_3Cl_{12}(C_6Me_6)_2$ taken with cross polarization [15]. (b) Variable-temperature ^{13}C CP/MASS spectrum of $U_3Cl_{12}(C_6Me_6)_2$; * denotes SSBs [16].

chemical shift is strongly temperature dependent. It is reasonable to assign this signal to the aromatic carbons as those carbons that are closest to the paramagnetic centers and are more likely to have appreciable chemical shift anisotropy. The static spectrum at room temperature is consistent with this interpretation as it shows the superposition of two powder patterns with different widths and similar isotropic values.

The application of variable-temperature MASS NMR to a somewhat more complicated magnetic phenomenon, antiferromagnetic exchange coupling [17,18], is illustrated in Fig. 8.14 which reports ^{13}C spectra of anhydrous Cu(II)*n*-butyrate. The X-ray structure shows two inequivalent types of carboxylate ligands thus causing the appearance of two sets of resonances in the ^{13}C NMR spectrum.

The antiferromagnetic interaction occurs through the electronic orbitals of ligands bridging the pair of metals (singlet state). There is, however, a triplet state a few hundred wavenumbers above the ground state. By increasing the temperature, electron-spin orientation gives rise to a maximum in the susceptibility curve near room temperature. The temperature dependence of the ^{13}C chemical shift reflects the variation of magnetic susceptibility in this antiferromagnetically coupled d^9–d^9 system as described in Eq. (5.8), which can be rewritten as

$$\delta_{obs} = \delta_{dia} + A \frac{g_e \mu_B}{\hbar \gamma_I kT} [3 + \exp(J/kT)]^{-1} \tag{8.7}$$

where J is the singlet–triplet energy separation and A is the hyperfine coupling constant for a given ^{13}C nucleus. The obtained J values for a number of anhydrous Cu(II) carboxylates agree quite well with those obtained from bulk magnetic susceptibility measurements. Furthermore, it is worthwhile to point out that such NMR determinations of J are not affected by the presence of traces of paramagnetic impurities as are bulk susceptibility measurements. The change in A moving along the alkyl chain is accounted for in terms of σ-delocalization of unpaired electron density into these carbon nuclei. This information sheds light on the mechanism of antiferromagnetic exchange coupling and may be of use in the development of magneto-structural correlations [18].

8.4.2. *Other nuclei MASS NMR*

There have been few reports in the literature dealing with the study of the effect of incorporating paramagnetic ions into diamagnetic solids in order to exploit their shift and relaxation properties as widely shown in solution. For instance ^{89}Y and ^{119}Sn (both spin $\frac{1}{2}$ nuclei) NMR spectra were obtained from a variety of solid solutions doped with paramagnetic Ln(III) ions [19,20]. The resulting spectra can be rationalized in terms of substitution of a paramagnetic ion for Y or Sn in the local coordination cage. This causes both a shift from the position of the diamagnetic resonance and a decrease in the spin-lattice relaxation times of spin-$\frac{1}{2}$ resonances. It is worthwhile to pinpoint that, since the relaxation times of nuclei close to paramagnetic ions are greatly reduced, the detection of these nuclei, which may be at a concentration less than 0.5% in these doped solids, became possible. Such a minor

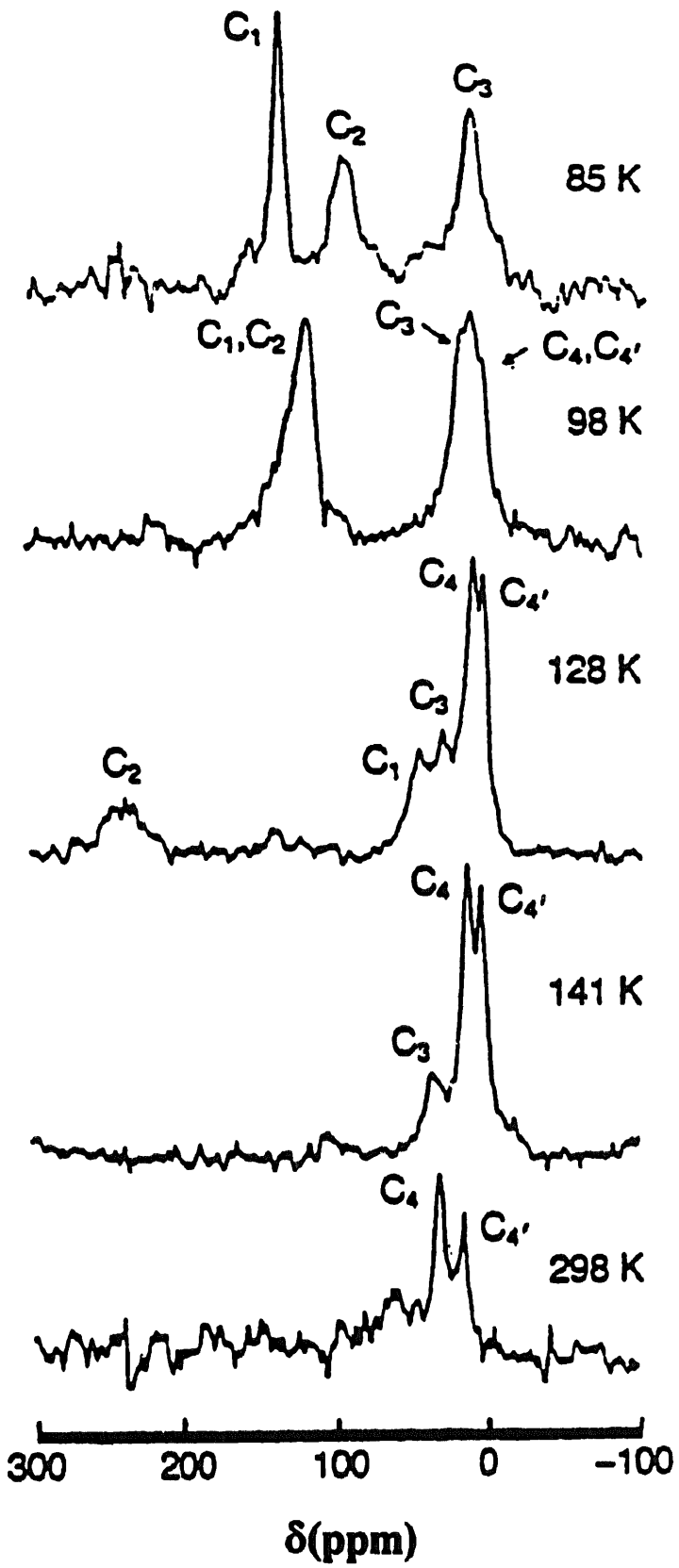

Fig. 8.14. Variable-temperature ^{13}C CP/MASS spectra of anhydrous copper(II) *n*-butyrate, a solid compound exhibiting antiferromagnetic exchange coupling. C_1 refers to carboxylate carbons, C_4 and $C_{4'}$ refer to methyl carbons, and C_2 and C_3 are the intermediate methylene carbons [18].

difference in the local environments could not have been distinguished by techniques such as X-ray diffraction!

As for the solution case, the isotropic shift of a paramagnetic compound contains contributions from three major terms, namely the diamagnetic term, the Fermi contact term and the pseudo contact (dipolar) term. Separation of contact and dipolar terms may be pursued by plotting the observed chemical shifts against the theoretical values of the contact (or dipolar) shift. Fermi contact interactions are usually the major contribution to the shifts observed in a series of rare-earth phosphates, vanadates and stannates. The large temperature effect on the ^{119}Sn chemical shift of $Nd_2Sn_2O_7$ and $Sm_2Sn_2O_7$ has suggested [21] their use as internal thermometers for the temperature calibration of MASS probes as an alternative to samarium acetate.

^{23}Na appears to be a particularly suitable nucleus to extract the spatial information contained in the SSB manifold in paramagnetic salts. In these systems the SSB envelope of Na^+ ions is essentially determined by the anisotropy in the dipolar term. Thus, analysis of the relative intensities of the SSBs [22] allows one to obtain the principal components of the shift tensor from which r distances from the paramagnetic center can be evaluated by applying the same method reported above for the ^{13}C resonances of Ln(III) acetates.

The large effect of magnetic materials on the properties of diamagnetic systems suggests that care should be exercised when dealing with the use of SSB patterns to obtain information on chemical structure. It has been shown [23] that the occurrence of only 1% in weight of the ferromagnetic oxide Fe_3O_4 (magnetite) causes extensive sideband formation in the ^{27}Al MASS NMR spectrum of an alumino silicate. Thus, especially if natural minerals are investigated, an overestimate of CSA may be caused by the broadening due to magnetic inclusions.

8.4.3. Caveats in MASS experiments

8.4.3.1. Matching the correct "magic" angle

By spinning a solid we impose a time dependence on all anisotropic nuclear interactions to achieve an averaging of these interactions. Let us consider a given internuclear r_{ij} vector which has an angle χ with respect to the axis of the cylindrical sample (Fig. 8.15). As rotation of the sample occurs along vector s, the angle γ for the nuclear i–j pair will vary between $\beta - \chi$ and $\beta + \chi$, where β is the angle between the axis of spinning and B_0. The extent of the narrowing effect on the NMR resonance will depend on $\langle 3\cos^2\gamma - 1\rangle$. Simple geometric arguments show that

$$\langle 3\cos^2\gamma - 1\rangle = (3\cos^2\beta - 1)(3\cos^2\chi - 1)/2$$

Now, χ can take all possible values between π and $-\pi$, whereas β is chosen by the experimentalist and, when it is equal to 54°44′ causes the "magic" effect, since for this angle $\cos\beta = 3^{-1/2}$. The average $\langle 3\cos^2\gamma - 1\rangle$ is then zero for all the initial values of χ. If the rotational angle β is adjusted to be close to the "magic" angle, but not exactly equal to it, we see then that the asymmetry is reduced only by the scale factor $F(\beta) = |(3\cos^2\beta - 1)/2|$.

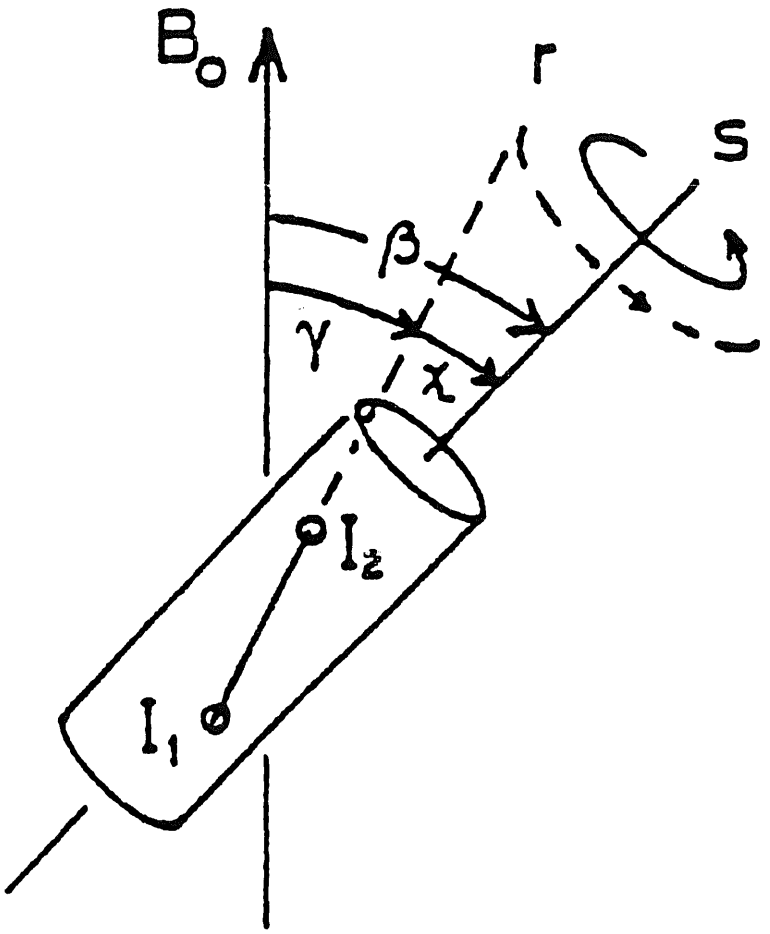

Fig. 8.15. Angles involved in MASS experiments.

8.4.3.2. Identification of the center band

The MASS spectra of paramagnetic compounds are characterized by a high number of SSBs. The first action the NMR spectroscopist may wish to take deals with the identification of the center band. Often, in the presence of large anisotropy the intensity of the center band may be very small. The easiest route to identify the center band consists of varying the spinning speed: the center band is the only resonance which is invariant to this parameter.

References

[1] C.A. Fyfe, Solid State NMR for Chemists, C.E.C. Press, Guelph, Ontario, Canada, 1983.
[2] B.R. McGarvey and S. Nagy, Inorg. Chem., 26 (1987) 4198.
[3] S.E. Anderson, J. Organomet. Chem., 71 (1974) 263.
[4] T. Sandreczki, D. Ondercin and R.W. Kreilick, J. Magn. Reson., 34 (1979) 171.
[5] A. Reuveni and B.R. McGarvey, J. Magn. Reson., 34 (1979) 181.
[6] G. Soda and T. Chiba, J. Chem. Phys., 50 (1969) 439.
[7] R.J. Wittebort, J. Magn. Reson., 83 (1989) 626.

[8] S.E. Woehler, R.J. Wittebort, S.M. Oh, D.N. Hendrickson, D. Inniss and C.E. Strouse, J. Am. Chem. Soc., 108 (1986) 2938.
[9] T.-H. Lin, J.A. Di Natale and R.R. Vold, J. Am. Chem. Soc., 116 (1994) 2133.
[10] C.J. Groombridge and M.J. Perkins, J. Chem. Soc. Chem. Commun., (1991) 1164.
[11] G.C. Campbell, R.C. Crosby and J.F. Haw, J. Magn. Reson., 69 (1986) 191.
[12] S. Ganapathy, V.P. Chacko, R.G. Bryant and M.C. Etter, J. Am. Chem. Soc., 108 (1986) 3159.
[13] A.N. Clayton, C.M. Dobson and C.P. Grey, J. Chem. Soc. Chem. Commun., (1990) 72.
[14] A.R. Brough, C.P. Grey and C.M. Dobson, J. Am. Chem. Soc., 115 (1993) 7318.
[15] B.J. Bleaney, J. Magn. Reson., 8 (1972) 91.
[16] J.F. Haw and G.C. Campbell, J. Magn. Reson., 66 (1986) 558.
[17] T.H. Walter and E. Oldfield, J. Chem. Soc. Chem. Commun., (1987) 646.
[18] G.C. Campbell and J.F. Haw, Inorg. Chem., 27 (1988) 3706.
[19] C.P. Grey, M.E. Smith, A.K. Cheetham, C.M. Dobson and R. Dupree, J. Am. Chem. Soc., 112 (1990) 4670.
[20] C.P. Grey, C.M. Dobson, A.K. Cheetham and R.J.B. Jakeman, J. Am. Chem. Soc., 111 (1989) 505.
[21] C.P. Grey, A.K. Cheetham and C.M. Dobson, J. Magn. Reson. A, 101 (1993) 299.
[22] A.R. Brough, C.P. Grey and C.M. Dobson, J. Chem. Soc. Chem. Commun., (1992) 742.
[23] E. Oldfield, R.A. Kinsey, K.A. Smith, J.A. Nichols and R.J. Kirkpatrick, J. Magn. Reson., 51 (1983) 325.